LINEAR ACCELERATOR FOR PRODUCTION OF TRITIUM: PHYSICS DESIGN CHALLENGES*

T. P. Wangler, G. P. Lawrence, T. S. Bhatia, J. H. Billen, K.C.D. Chan, R. W. Garnett, F. W. Guy, D. Liska, S. Nath, G. H. Neuschaefer, and M. Shubaly,
Los Alamos National Laboratory, Los Alamos, NM 87545

Introduction

In the summer of 1989, a collaboration between Los Alamos National Laboratory and Brookhaven National Laboratory conducted a study to establish a reference design of a facility for accelerator production of tritium (APT). The APT concept[1,2] is that of a neutron-spallation source, which is based on the use of high-energy protons to bombard lead nuclei, resulting in the production of large quantities of neutrons. Neutrons from the lead are captured by lithium to produce tritium. This paper describes the design of a 1.6-GeV, 250-mA proton cw linear accelerator for APT.

Reference Accelerator Configuration

The reference accelerator configuration (Fig 1) consists of two low-energy, 350-MHz, 125-mA proton linacs, whose beams are funneled at 20 MeV and injected into a single 700-MHz, 250-mA linac for acceleration to 1600 MeV. Each dc injector consists of a duoPIGatron ion source and low-energy beam transport (LEBT) line, which produces a 140-mA beam for injection into a radiofrequency-quadrupole (RFQ) linac structure. The RFQ focuses and adiabatically bunches the injected beam, and with the same rf electric fields accelerates the beam to an energy of 2.5 MeV. At this energy the drift-tube linac (DTL), which provides more efficient acceleration, and focusing from electromagnetic quadrupoles inside the drift tubes, increases the beam energy to 20 MeV. The two 20-MeV, 350-MHz beams arrive out of phase at an rf deflector element, which funnels them into a single colinear 700-MHz bunched beam for further acceleration in a high-energy, 700-MHz, 250-mA coupled-cavity linac (CCL) to the final energy of 1600 MeV.

The APT linac is designed with minimizing beam loss as first priority and efficiency as second priority. Radiation-hard electromagnetic quadrupoles are used in the drift tubes rather than permanent-magnet quadrupoles because of concerns about radiation damage. The size of electromagnetic quadrupoles imposes an upper limit on the choice of DTL frequency. A $2\beta\lambda$-type DTL is chosen to accomodate the physical length of the quadrupoles. For performance reasons, a two-frequency linac design is employed: 350 MHz for the RFQ and DTL, and 700 MHz for the CCL. Beam funneling is employed because it results in improved beam quality and reduced particle losses in the CCL for the desired current level. The CCL is designed in a modular fashion with the lattice units identified as types 1 to 7. Type 1 is composed of 2-cell lattice units; the number increases to 10 cells per lattice unit for Type 7. Overall there are 1451 lattice units in the CCL, with a total of 10275 accelerating cells. If necessary, an emittance filter, a system of collimators to remove beam halo, can be installed at 40 MeV after the major accelerator transitions. Lengths, rf power to the structure, and beam power are shown in Fig. 1 for each type of accelerating structure. A table within the figure provides an estimate of the number of rf tubes: 470 at 700 MHz and 12 at 350 MHz. A second table gives transverse and longitudinal emittances for a nonideal beam case used in the simulations, in which the beam is

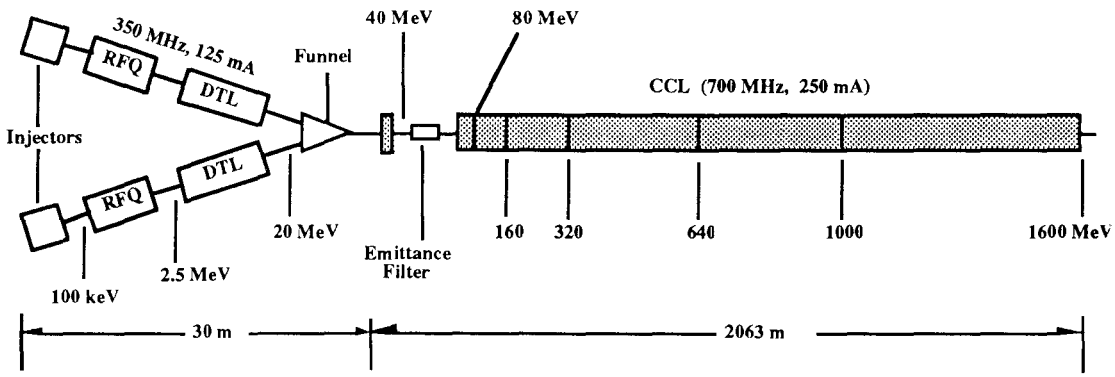

	Length (m)	RF Power (MW) Copper	Beam	Total	# RF Tubes
RFQ	3.4	0.4	0.3	0.7	2
DTL	11.3	1.3	2.2	3.5	10
CCL	2063	114.8	395.0	509.8	470
Total	2100	118.2	400.0	518.2	482

Total AC Power for Accelerator = 910 MW
(Assuming ac → beam efficiency = 0.49)

	Trans. Emittance* (π cm-mrad) Input	Output	Long. Emittance* (10^{-6}π eV-sec) Input	Output
RFQ	0.020	0.023	0.0	1.4
DTL	0.027	0.058	1.6	3.0
CCL	0.061	0.068	2.9	4.4

* Emittance values are for non-ideal beam.

Fig. 1. The APT reference accelerator configuration.

*Work supported by the US Department of Energy with Los Alamos National Laboratory Development funds.

deliberately mismatched to the DTL. Designing with a nonideal beam provides a safety margin, especially for considerations associated with beam loss.

We have chosen 350 MHz and 700 MHz for the APT reference design. The optimum choice of frequencies involves many issues, and we believe complete designs at different frequencies would be necessary to rigorously establish the best choice for APT. High frequencies distribute the total charge in more bunches and produce less space-charge-induced growth of emittance and halo. But at higher frequency the transverse dimensions decrease, and alignment and steering become more difficult. Furthermore, the apertures must decrease at higher frequency to avoid a high penalty in structure power efficiency, and at high frequency, nonlinear fields in the rf gaps reduce the usable apertures. On the basis of linac design experience, we believed that a choice of frequency much higher than 350/700 MHz would result in diminishing returns with respect to growth of emittance and halo and would probably significantly increase the problems associated with higher frequency. Low frequencies have the advantage of allowing larger apertures but generally result in larger beam size and more particles in fewer bunches, which translates into undesirable space-charge-induced growth of emittance and halo. Furthermore, lower frequencies require accelerating structures with larger transverse dimensions. The mechanical design and handling of very large and heavy components can make fabrication and precise alignment difficult. The German Spallations-Neutronenquelle (SNQ) design study[3] used frequencies of 100/200 MHz, which are the lowest values that we considered in the APT study. Comparison of SNQ with APT simulation results shows that SNQ had significantly more emittance growth than APT, which was not offset by the larger apertures (i.e., the aperture-to-rms ratios are larger for APT). For a definitive conclusion, a systematic study should be undertaken, using one linac-design approach. For the moment, we believe the evidence suggests that our choice of 350/700 MHz for APT is not far from optimum.

Linac Design Approach

Linac Design Philosophy

The main design objective for the APT linac is to provide high beam transmission and low particle losses to minimize radioactivation of the accelerator. A twofold strategy is used in the design. First, we establish good beam quality in the low-energy accelerators to minimize beam emittances (phase-space area) and halo. This is accomplished by (1) operating in a cw mode to reduce the peak current and the related space-charge effects, (2) using the RFQ for low-velocity bunching and acceleration, (3) using ramped accelerating fields in the DTL to control the longitudinal distribution, (4) funneling to provide the desired current at lower emittance, and (5) using high-frequency accelerating structures to reduce the charge per bunch and the undesirable nonlinear space-charge forces that cause halo growth. Second, in the high-energy linac we try to keep the beam away from radial apertures and longitudinal bucket limits and to reduce beam losses that cause activation. This is accomplished by providing (1) a large aperture to rms-beam-size ratio, (2) a large bucket (separatrix) width to rms-bunch-length ratio, (3) good alignment and beam steering, and (4) good phase control of the accelerator structures. Activation and radiation damage effects from residual halo and beam losses can be limited by (1) using radiation-hard electromagnetic quadrupoles wherever possible, (2) restricting the major transitions (bunching and frequency doubling) to the lowest velocities, where the associated local beam losses have minimal activation effects, and (3) using emittance filters after the major transitions to remove halo that leads to particle losses.

It is important to control the growth of emittance and the associated beam halo to reduce beam losses. Although the causes of beam halo formation in phase space are not completely understood, we have observed in numerical simulation studies that nonlinear space-charge forces act to produce halo. Nonlinear space-charge forces at transitions in the accelerator, where parameters change, appear to increase the amount of halo. Transitions such as changes in the strength of the external focusing force, changes in periodicity of the focusing lattice, introduction of deflecting elements, or changes in rf frequency cause a change in the external focusing, and the beam must adapt. Given a sufficient number of beam-plasma periods after such a transition is introduced, the beam has evolved to a quasi-stationary state. During this evolution process, beam halo is produced. The time scale for halo production is not yet well established but appears to be in the range of a few to a few tens of beam-plasma periods. This time scale may be relevant to the design of emittance-filter systems. It does appear that accelerator transitions should be introduced only when necessary; for example, ion source extraction, bunching, and (in some cases) funneling require accelerator transitions. If these transitions are kept at the low-energy end of the accelerator, the activation effects of the associated local beam losses are minimized, and collimator systems that act as emittance filters to remove the halo will be more effective and easier to implement. Good beam matching across these transitions is very important to minimize the disruption to the beam. With regard to rms emittance, we believe this is a quantity whose growth should be controlled. Not only is rms-emittance growth often correlated with halo production, but the rms emittance affects the overall spatial size of a given beam distribution; the larger the rms emittance, the larger the beam size and the greater the extension in real space of the halo that already exists.

Radio-Frequency Quadrupole

The RFQ design parameters are shown in Table 1. The RFQ bunches the 140-mA input dc beam and accelerates it from 0.1 to 2.5 MeV. The output beam from the RFQ is then injected into the following DTL using a matching section, which consists of four electromagnetic quadrupole magnets and two rf buncher cavities. The beam transmission, output current, and output emittances for the RFQ are based on the results of numerical simulation with the PARMTEQ code. By using a vane geometry with constant transverse radius of curvature, we expect a maximum peak surface electric field of about 1.8

TABLE 1
APT RFQ Parameters

Frequency	350 MHz
Energy	0.1 to 2.5 MeV
Synchronous phase	-90° to -37°
Vane modulation	1.0 to 1.8
Radial aperture (a)	0.375 to 0.310 cm
Intervane voltage	95 kV
Peak surface field	33 MV/m
DC injection current	140 mA
Output current	128 mA
Beam transmission	0.91
Transverse rms emittance	0.020 to 0.023 π cm-mrad
Longitudinal rms emittance	0.0 to 1.4 x 10^{-6} π eV-s
RFQ length	3.4 m
Copper power	0.4 MW
Beam power	0.3 MW
Total power	0.7 MW

times the Kilpatrick value, which corresponds to 33-MV/m. The current limit is 250 mA, and we used a constant-current-limit accelerating section to reduce the RFQ length for easier tuning. The RFQ cavity can be driven with a single 350-MHz klystron.

Drift-Tube Linac

The DTL parameters are shown in Table 2. The DTL uses a FODO focusing lattice composed of radiation hard electromagnetic quadrupole magnets inside the drift tubes and a $2\beta\lambda$ cell to provide sufficient room for the magnets. The quadrupole magnets require a gradient of 46-T/m and an effective length of 6.4 cm, which results in a zero-current betatron phase advance per focusing period of $\sigma_0 = 70°$. The DTL can be configured in five separate rf tanks, each of which can be driven from a single 350-MHz klystron. The output emittances listed in Table 2 are conservative values, obtained from numerical simulation using the PARMILA code for a nonideal case where the beam is deliberately mismatched to the DTL.

Funnel

Table 3 shows the parameters of the funneling system for APT. The beams are focused transversely with electromagnetic quadrupole magnets and longitudinally with 350-MHz rf-buncher cavities. As the beams approach the common final axis, the spacing becomes small, and more compact permanent-magnet quadrupoles and 700-MHz buncher cavities are required. Finally, the beams are merged in an electromagnetic quadrupole that is horizontally defocusing and passed into the 350-MHz rf deflector. The deflector phase is chosen so that the transverse rf fields act on the two out-of-phase bunched beams to produce the final beam, which is injected into the 700-MHz linac.

TABLE 2.
APT DTL Parameters

Structure	$2\beta\lambda$
Lattice	FODO
Frequency	350 MHz
Energy	2.5 to 20 MeV
Transverse rms emittance	0.027 to 0.058 π cm-mrad
Longitudinal rms emittance	1.6 to 3.0 x 10^{-6} π eV-s
Synchronous phase	-40°
Accelerating gradient (E_0T)	1.1 to 3.1 MV/m
Peak surface field	22 MV/m
Radial aperture	0.84 cm
Length	11.3 m
Number of cells	51
Copper power	1.3 MW
Beam power	2.2 MW
Total power	3.5 MW

TABLE 3.
APT Funnel Parameters

Energy	20 MeV
Number of quadrupoles	2 x 5 + 2 = 12
Number of dipoles	2 x 2 = 4
Number of bunchers	2 x 2 = 4
Number of rf deflectors	1
Length	1.5 m
Initial beam separation	60.5 cm
Aperture radius	0.8 cm
Input beam current	2 x 125 mA
Output beam current	250 mA
Transverse rms emittance	0.058 to 0.061 π cm-mrad
Longitudinal rms emittance	3.0 to 3.0 x 10^{-6} π eV-s
Copper rf power	0.25 MW

Coupled-Cavity Linac

The CCL parameters are summarized in Table 4. The longitudinal phase advance for zero current ranged from 15° at the CCL entrance to 3.4° at the end. The transverse phase advance for zero current was held constant at 70°.

TABLE 4.
APT CCL PARAMETERS

Structure	Side-Coupled
Lattice	FODO, 7 Sections
Frequency	700 MHz
Energy	20 - 1600 MeV
Current	250 mA
Transverse rms emittance	0.061 to 0.068 π cm-mrad
Longitudinal rms emittance	3.0 to 4.4 x 10^{-6} π eV-s
Number per bunch	2.2 x 10^9
Accelerating gradient (E_0T)	1 MV/m (lattice average)
Peak surface field	7.2 MV/m
Aperture radius	1.4 - 3.5 cm
Synchronous phase	-60° to -40°
Length	2063 m
Number of lattice Units	1451
Cells/tank	2,3,4,6,8,10
Copper power	115 MW
Beam power	395 MW
Total rf power	510 MW

To provide strongest focusing in the CCL, we have chosen to use relatively short tanks with a singlet FODO lattice, ensuring a high density of focusing elements. To guarantee a large transit-time factor and better stability against adverse effects from excitation of high-order modes, we have designed each tank length to correspond to the

correct local value of velocity (β). Having different sections in the CCL allows us to optimize the linac parameters for each velocity region. A relatively small number of sections results in fewer different component parameters (e.g., aperture size, quadrupole parameters, rf-module designs, etc.), which facilitates fabrication of the accelerator. This feature must be balanced against the advantage of keeping the parameter changes small from section to section to avoid introducing significant transitions that can disturb the beam equilibrium and cause growth of halo and additional beam spill. We chose seven CCL sections for the APT reference design. We chose a large radial aperture within each velocity region and limited the aperture to a value of about $\beta_i\lambda/2\pi$, where β_i is the initial velocity of the section, to avoid a large reduction in transit-time factor. Additional design studies may allow us to determine whether this criterion is necessary. We chose the number of cells per tank, and the corresponding focusing lattice period, in each section to ensure a large value of aperture to rms-beam-size ratio calculated from a 3-dimensional uniform ellipsoid model. Although the choice of short tanks is desirable to maintain strongest focusing, this requires a larger number of component tanks to achieve the full energy gain.

We examined the effects of high-order-mode excitation by the beam (beam breakup) for the CCL reference design. The most serious effect is generally associated with excitation of a cavity dipole mode, usually the TM_{110} mode, by an off-axis beam; this effect occurs above a certain threshold in beam current. When the cavity dipole mode is excited, it exerts a transverse force on the beam. The TM_{110}-mode frequency is not harmonically related to the accelerating-mode frequency, and after an initial transient buildup, the final beam is subject to a time-dependent deflection, which causes an effective jitter of the beam centroid. Consequently, the envelope of the output transverse phase-space distribution is enlarged, when averaged over time, and the effective emittance is increased. This problem has been of concern for high-current electron linacs, but we conclude that it is not serious for the APT CCL for two reasons: first, the proton is nearly 2000 times more massive than the electron, which reduces the deflection for a given cavity-excitation level. This greater inertia of the proton provides stabilization against deflection. Second, the design velocity of the cavities increases from tank to tank in the APT CCL (the proton dynamics are not in the extreme relativistic region, as are the electron dynamics in most electron linacs). Although the accelerating-mode frequency is the same for all tanks, the TM_{110}-dipole mode frequency differs from tank to tank. This difference makes the growth of a significant TM_{110} amplitude difficult because a TM_{110} deflection of the beam from a given tank is not able to drive a TM_{110} excitation in subsequent cavities. A TM_{110} frequency mismatch can be increased, if necessary, during tuning of the cavities to ensure that the TM_{110}-mode excitation causes no significant emittance growth.

APT Numerical Simulation Calculations

The numerical simulation codes used consist of PARMTEQ for the RFQ, PARMILA for the DTL and funnel, and CCLDYN for the CCL. These codes track particles through the accelerator, and most treat the space-charge forces using a fast 2-dimensional particle-in-cell approach. In each time step, the particles are allocated to cells of an r-z mesh, and space-charge fields are calculated and used together with the external forces to advance the particles for the next step. In the funnel, where the average x- and y-plane beam envelopes are not symmetrical, a 3-dimensional space-charge calculation is used. We carried out the simulation studies for APT with an initial matched Gaussian dc beam using 7500 particles into the RFQ. (The measured beam from relevant dc injectors is consistent with a Gaussian profile). The input beam is distributed uniformly in the longitudinal direction and is assigned zero initial energy spread (a good approximation for the 10-to 100-eV energy spread of a real beam). We did simulation studies for two cases: an ideal beam case and a nonideal beam case. For the ideal beam case, all linac fields were set to their design values, and the matching quadrupoles and rf cavities preceding the DTL and CCL were set to provide an ideal match as determined by the program TRACE3D. (Matching into the CCL is provided by beam elements of the funnel line, and matching into the DTL, by a special matching section composed of four quadrupole lenses and two rf cavities.) The nonideal APT beam differs from the ideal beam in that we changed parameters in the matching section before the DTL to produce a large mismatch. Although we believe the nonideal beam represents a more realistic representation of the typical beam quality that has been obtained in previous high-energy linacs, it may be possible to improve the performance from that of the nonideal case, especially by providing and using the information from high-performance beam diagnostics.

The simulation results for the nonideal beam are shown in Figure 2. The upper figures show transverse displacement versus angle (x versus x' and y versus y'). The lower right figure shows the energy versus phase relative to the design particle (longitudinal phase space). The stable longitudinal region is also shown in the lower right figure for

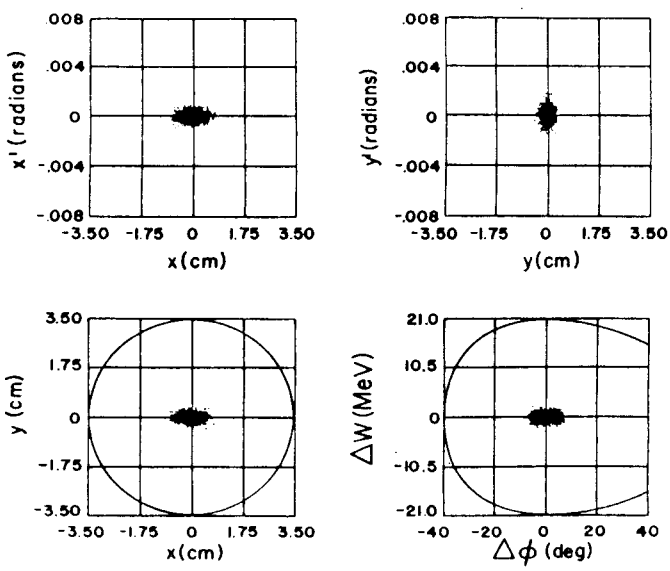

Fig. 2. Output beam at 1600 MeV from the numerical simulation for the nonideal beam case.

TABLE 5.
Beam Loss Estimates in APT CCL Based on Extrapolation Procedure Using Simulation Results

Energy (MeV)	20	40	80	160	320	640	1000
Peak loss (nA/m)	3000	20	0.06	0.06	0.06	0.06	0.06
Distributed loss (nA/m)	80	0.4	0.001	0.001	0.001	0.001	0.001

TABLE 6.
Activation Estimates from the Simulation Results

Energy (MeV)	20	40	80	160	320	640	1000
Peak (mRem/h)	48	1.6	0.024	0.12	0.48	0.96	1.4
Distributed (mRem/h)	1.3	0.032	0.0004	0.002	0.008	0.016	0.024

comparison with the particles. The lower left figure shows the x-versus-y cross section and the circular output aperture for the final beam. The space occupied by the beam in the CCL is much smaller than the acceptance limits, which was a main objective of the design. Beam emittances for the nonideal beam simulation are given in Fig. 1 and Tables 2 through 4. The aperture to rms-beam-size ratio in the CCL ranged from 20 to 31 for the ideal beam and from 14 to 22 for the nonideal beam. Thus, above 20 MeV, the design procedure succeeded in obtaining large aperture to rms -beam-size ratios.

To arrive at an initial estimate of losses in the reference design, we have adopted an extrapolation procedure, which we have applied to the nonideal beam simulation. In this procedure, we obtained beam loss values in each section of the CCL for reduced values of the aperture. We extrapolated these loss values to an effective aperture that we chose to be two standard deviations (3.4 mm) less than the true aperture, to account for estimated beam mis-steering. In cases where the extrapolated numbers were too small to be significant, we used upper-limit values for the extrapolation to provide a conservative estimate. The results are shown in Table 5. We conservatively obtained the peak-loss estimates by reassigning all the losses of a section to the first four cells of the section, where the highest losses are observed in the simulation. We obtained the distributed-loss estimate by artificially distributing all lost particles of a section in a uniform loss distribution. Thus, in obtaining these estimates, we used the same extrapolated lost particles for both the peak and distributed losses. We believe our procedures should result in upper bounds of simulation code prediction for losses for each type. The corresponding activation levels can be estimated if (1) we take the rule-of-thumb from the Los Alamos Meson Physics Facility (LAMPF) that 1 nA/m loss results in 20 mrem/h activation at 800 MeV, and (2) we assume that the activation level as a function of energy is proportional to the yield of neutrons per incident proton in copper (which depends nearly linearly on proton energy above 500 MeV). The results, shown in Table 6, are that the most radioactive area is at the entrance to the CCL, which may require remote maintenance for certain jobs. Except for this one place, the activation levels would be no more than a few mrem/h, which is acceptable for hands-on maintenance.

Our goal has been to produce a conservative reference design with a compact, high-quality beam and low beam losses. We used numerical simulation studies, which included space charge, to confirm the good beam characteristics of this reference design.

Acknowledgments

The APT reference design was carried out by many people at Los Alamos, whose efforts and ideas we acknowledge. We thank M. Lynch and P. J. Tallerico, who are responsible for the rf-system design, and B. Blind and A. J. Jason, who are responsible for the high-energy optics design, neither of which was discussed in this paper. We acknowledge the critical evaluation of the design ideas by S. Schriber, A. Browman, and R. Jameson, and thank R. Burick for his support and encouragement.

References

1. M. T. Wilson, T. S. Bhatia, F. W. Guy, G. H. Neuschaefer, T. P. Wangler, and L. M. Young "Accelerator for the Production of Tritium (APT), Proc. of the 1989 Particle Accelerator Conference, 761 (1989).
2. "Accelerator Production of Tritium APT," Brookhaven National Laboratory report BNL/NPB-88-143 (1989).
3. Clemens Zettler,"The Linear Accelerator and Pulse Compressor of the SNQ Project," Proceedings of the 1984 Linear Accelerator Conference, Gesellschaft fur Schwerionenforschung, GSI Report-84-11, 480 (1984).